12-1-1999

Multimode Solution for the Reflection Properties of an Open-Ended Rectangular Waveguide Radiating into a Dielectric Half-Space: The Forward and Inverse Problems

R. Zoughi
Missouri University of Science and Technology, zoughi@mst.edu

Aaron D. Benally

Karl Joseph Bois

Recommended Citation

R. Zoughi et al., "Multimode Solution for the Reflection Properties of an Open-Ended Rectangular Waveguide Radiating into a Dielectric Half-Space: The Forward and Inverse Problems," *IEEE Transactions on Instrumentation and Measurement*, vol. 48, no. 6, pp. 1131-1140, Institute of Electrical and Electronics Engineers (IEEE), Dec 1999.
The definitive version is available at https://doi.org/10.1109/19.816127

Multimode Solution for the Reflection Properties of an Open-Ended Rectangular Waveguide Radiating into a Dielectric Half-Space: The Forward and Inverse Problems

Karl J. Bois, *Member, IEEE*, Aaron D. Benally, and Reza Zoughi, *Senior Member, IEEE*

***Abstract*—Open-ended rectangular waveguides are extensively used in nondestructive dielectric material evaluation. The dielectric properties of an infinite-half space of a material are calculated from the measured reflection properties referenced to the waveguide aperture. This calculation relies on a theoretical and numerical derivation of the reflection coefficient likewise referenced to the waveguide aperture. Most of these derivations assume the dominant mode field distribution across the waveguide aperture. However, when dealing with low permittivity and low loss dielectric materials, there may exist significant errors when calculating the dielectric properties from the measured reflection coefficient. These errors have also shown to be more significant in the upper frequency portion of a waveguide band. More accurate results are obtained when higher-order modes are considered in addition to the dominant waveguide mode. However, most studies incorporating higher-order modes have used various approximations when calculating the reflection properties and have not provided a full discussion on the influences of dielectric properties of the infinite-half space and the frequency of operation. This paper gives a rigorous and exact formulation in which the dominant mode and the evanescent higher-order modes are used as basis functions to obtain the solution for the reflection coefficient at the waveguide aperture. The analytic formulation uses Fourier analysis in addition to the forcing of the necessary boundary conditions at the waveguide aperture. The solution also readily accounts for the complex contributions of both TE and TM higher-order modes. Finally, the influences of the dielectric properties of the infinite-half space and the frequency of operation are investigated.**

***Index Terms*—Dielectric constant, half-space, inverse problem, modal solution, waveguide.**

I. Introduction

In the past few decades, open-ended rectangular waveguide sensors have proven to be versatile probes in numerous microwave and millimeter wave inspection applications. Initially used as a probe to study the behavior of antennas on space vehicles on reentry into earth's atmosphere, they are now the workhorse of many nondestructive testing and evaluation applications. These applications include dielectric material property measurement and characterization [1]–[5], thickness measurement of dielectric slabs and detection of disbonds and delaminations in stratified dielectric composites [6], [7], porosity level estimation in plastics and composites [8], detection of hairline cracks in metal surfaces [9], characterization of concrete based materials [10], [11] and medical applications [12]. Customarily, the reflection coefficient at the aperture of the waveguide, Γ, is measured or calculated as a function of the operating frequency and the dielectric and geometrical properties of the medium under test [6]. When calculating Γ, the relationship describing the coupling of the fields launched from the waveguide aperture into the medium under test must be found.

To this end, many studies have dealt with the special case of radiation into an infinite half-space of a dielectric material. This particular case was first studied employing variational methods in which the field distribution at the aperture of the waveguide is approximated to that of the dominant TE_{10} mode in the waveguide [13], [14]. These derivations are sufficiently accurate and computationally efficient for many practical applications. However, when using these derivations to recalculate the dielectric properties of a low permittivity and low loss dielectric half-space from the measured Γ, significant errors may result which are also shown to be frequency dependent [10]. Since previous publications dealing with the reflection properties of an open-ended waveguide probe were for the most part performed at a single frequency and for the particular case of a half-space of air, this important behavior has not been fully investigated. These errors are primarily attributed to the exclusion of higher-order modes, present at the waveguide aperture in the theoretical derivation of Γ. Consequently, the inclusion of higher-order modes for these types of applications has been proposed by several investigators [1], [2], [15]–[19], [21]. Although offering a more rigorous solution to the problem, the contributions of both the electric and magnetic hertzian potential (e.g., both TM and TE higher-order modes or cross-polarization) have not always been included in the theoretical formulations such as those presented in [1], [2], and [15]. This provides for some degree of calculation simplification and for some applications renders acceptable results. In an attempt to include the influence of

Manuscript received January 15, 1999; revised September 2, 1999. This work was supported by the joint National Science Foundation under Contract CMS-9523264 and the Electric Power Research Institute under Contract WO 8031-09, Program on Sensor and Sensor Systems and Other Dispersed Civil Infrastructure Systems.

K. J. Bois is with the Packaging Group, VLSI Technology Center, Hewlett-Packard Company, Fort Collins, CO 80528 USA.

A. D. Benally and R. Zoughi are with the Applied Microwave Nondestructive Testing Laboratory, Electrical Engineering Department, Colorado State University, Fort Collins, CO 80523 USA.

Publisher Item Identifier S 0018-9456(99)09239-6.

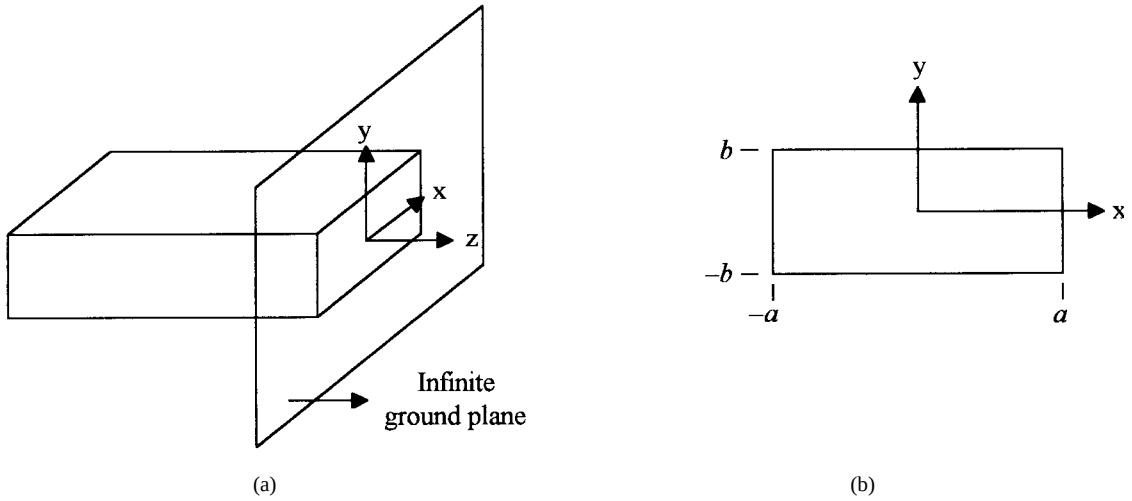

(a) (b)

Fig. 1. Open-ended waveguide radiating into infinite half-space: (a) side view and (b) front view (not showing the ground plane).

higher-order modes, others have applied many different mathematical formulations attributed to different physical models of their particular applications. These have included the variational methods [1], [2], [18], [19], integral formulations [3], [15]–[17], [20], matrix correlation methods [21], [22] as well as method of moments [23]–[24]. All of the studies that have included both the TE and the TM higher-order modes, except in [3], require some form of numerical or theoretical approximation in order to solve for the unknown coefficients that lead to the final solution for a given set of modes.

Most studies of open-ended waveguide probes have primarily dealt with its radiation properties into an infinite half-space of free-space. Reference [3] gives a concise solution to the reflection properties of an open-ended rectangular waveguide radiating into an infinite half-space of a dielectric. However, it provides for no discussions as to the reasons behind the choice of higher-order modes that have been included in its final solution. In addition, it does not discuss the influence that the dielectric properties of the infinite half-space and the frequency of operation have on the choice of higher-order modes. In [23], although not for the case of an infinite half-space, only a limited number of higher-order modes are used in the derivation without a clear indication as to why they have been chosen (as a function of frequency and the dielectric properties of the medium). In this paper, the important issue of the choice of higher-order modes as a function of frequency and the dielectric properties of the half-space is fully addressed, particularly as it relates to the inverse problem (i.e., recalculating the dielectric properties of the half-space).

This paper gives a rigorous and exact formulation in which the dominant mode and the evanescent higher-order modes are used as basis functions to obtain the solution for the reflection coefficient, Γ, at the waveguide aperture. The analytic formulation uses Fourier analysis similar to that used in [20], in addition to the forcing of the necessary boundary conditions at the waveguide aperture. Reference [20] deals with the radiation of a rectangular waveguide with a coated lossy flange into free-space. However, the formulations outlined in this paper, although similar to those in [20], are modified to account for the problem of radiation of an open-ended waveguide into a generally lossy dielectric half-space. The resulting solution is simplified to produce a set of equations that requires straightforward numerical evaluation. The solution also readily accounts for the complex contributions of both TE and TM higher-order modes. In this approach only a set of higher-order modes necessary to obtain convergence is included in the formulation. The contribution of these higher-order modes will be discussed as a function of the dielectric properties of the infinite half-space, and the frequency of operation followed by some measurements for comparison with other techniques (i.e., [18]). Since the main justification for this theoretical effort is the inverse problem in which the dielectric properties of the infinite half-space are recalculated using this formulation in conjunction with the measured values of Γ, a brief discussion will be devoted to this topic as well.

II. Integral Solution

The geometry of the problem is illustrated in Fig. 1 in which an open-ended rectangular waveguide with its broad dimension $2a$ and narrow dimension $2b$ is mounted on an infinite ground plane, and is radiating into an infinite half-space of a dielectric material. The complex relative dielectric constant of the half-space is given by $\varepsilon_r = \varepsilon_r' - j\varepsilon_r''$. As mentioned earlier, ε_r' and ε_r'' are referred to as the relative permittivity and loss factor of the material, respectively. Loss tangent, $\tan\delta$, is the ratio of the permittivity to loss factor $(\varepsilon_r''/\varepsilon_r')$.

In the following derivations a harmonic time variation of the type $(e^{j\omega t})$ is assumed in addition to the fact that the waveguide walls are assumed to be perfect conductors. Consider that the waveguide is operating in its dominant TE_{10} mode, and that the incident fields inside the waveguide $\bar{E}^i$ and $\bar{H}^i$ are derived, using Maxwell's equations [25], from the magnetic hertzian vector $\bar{\Pi}^{ih} = \Pi^{ih}\hat{z}$ given by

$$\Pi^{ih}(x,y,z) = \frac{A^i}{k_o^2\eta_o}\cos a_1(x+a)e^{-jk_{10}z} \tag{1}$$

where $\hat{z}$ is the unit vector in the z-direction, $\eta_o = \sqrt{\mu_o/\varepsilon_o}$ is the free-space intrinsic impedance, $k_o = \omega\sqrt{\varepsilon_o\mu_o}$ is the free-space wavenumber and ε_o and μ_o are the permittivity and permeability of free-space, respectively and ω is the radial frequency. Also, the superscript i designates fields incident on the aperture, and superscript h refers to constants and functions associated with the magnetic potential vector. The reflected fields inside the waveguide, $\bar{E}^r$ and $\bar{H}^r$, are derived from the electric and magnetic Hertzian vectors $\bar{\Pi}^{re} = \Pi^{re}\hat{z}$ and $\bar{\Pi}^{rh} = \Pi^{rh}\hat{z}$ as

$$\Pi^{re}(x,y,z) = \sum_{m,n=1}^{\infty} \frac{A^e_{mn}}{k_o^2} \sin a_m(x+a) \sin b_n(y+b) e^{jk_{mn}z} \quad (2)$$

$$\Pi^{rh}(x,y,z) = \sum_{\substack{m,n=0 \\ m=n\neq 0}}^{\infty} \frac{A^h_{mn}}{k_o^2\eta_o} \cos a_m(x+a) \sin b_n(y+b) e^{jk_{mn}z} \quad (3)$$

where $a_m = (m\pi/2a)$, $b_n = (n\pi/2b)$, $k_{mn} = \sqrt{k_o^2 - a_m^2 - b_n^2}$ and A^e_{mn} and A^h_{mn} are the sought for unknown coefficients. Also, the superscript r designates fields reflected back from the aperture, and superscript e refers to constants and functions associated with the electric potential vector. The fields in the dielectric half-space ($\bar{E}^t$ and $\bar{H}^t$) can be derived by the electric and magnetic Hertzian vectors $\bar{\Pi}^{te} = \Pi^{te}\hat{z}$ and $\bar{\Pi}^{th} = \Pi^{th}\hat{z}$ in the following form:

$$\Pi^{re}(x,y,z) = \frac{1}{4\pi^2}\int_{-\infty}^{\infty}\int_{-\infty}^{\infty} \frac{A^e(\xi,\eta)}{k_1^2} e^{-j(\xi x+\eta y+\zeta z)}\, d\xi\, d\eta \quad (4)$$

$$\Pi^{rh}(x,y,z) = \frac{1}{4\pi^2}\int_{-\infty}^{\infty}\int_{-\infty}^{\infty} \frac{A^h(\xi,\eta)}{k_1^2\eta_1} e^{-j(\xi x+\eta y+\zeta z)}\, d\xi\, d\eta \quad (5)$$

where $\zeta = \sqrt{k_1^2 - \xi^2 - \eta^2}$, $k_1 = k_o\sqrt{\varepsilon_r\mu_r}$, $\eta_1 = \eta_o\sqrt{\mu_r/\varepsilon_r}$ and $A^{e,h}(\xi,\eta)$ are unknown spectral functions in the wavenumber domain and μ_r is the relative permeability of the medium. The half-space herein will be assumed nonmagnetic (i.e., $\mu_r = 1$). It should be noted that a branch cut is chosen such that $\Re e(\zeta) \geq 0$ and $\Im m(\zeta) \leq 0$ so that $\bar{\Pi}^{te,tm}$ represent forward propagating waves in the z^+-direction since there is no physical mechanism to produce backward propagating waves in the dielectric half-space. It can be easily shown that $\bar{\Pi}^{te,tm}$ satisfies the wave equation

$$\left(\nabla^2 + k_1^2\right)\bar{\Pi}^{te,tm} = 0 \quad (6)$$

In all regions, the fields can be related to the Hertzian vector by the following relationships:

$$\bar{E} = \bar{\nabla}(\bar{\nabla}\cdot\bar{\Pi}^e) + k_1^2\bar{\Pi}^e - j\omega\mu\bar{\nabla}\times\bar{\Pi}^h \quad (7)$$

$$\bar{H} = \bar{\nabla}(\bar{\nabla}\cdot\bar{\Pi}^h) + k_1^2\bar{\Pi}^h + j\omega\varepsilon\bar{\nabla}\times\bar{\Pi}^e \quad (8)$$

where $\varepsilon = \varepsilon_o\varepsilon_r$ and $\mu = \mu_o$. At the waveguide aperture ($z = 0$), the following boundary conditions must be satisfied

$$E^t_{x,y} = \begin{cases} E^i_{x,y}(x,y,0) + E^r_{x,y}(x,y,0) & |x| \leq a, \quad |y| \leq b \\ 0 & \text{elsewhere} \end{cases} \quad (9)$$

$$\bar{H}^t_{x,y} = \bar{H}^i_{x,y}(x,y,0) + \bar{H}^r_{x,y}(x,y,0) \quad |x| \leq a, \quad |y| \leq b. \quad (10)$$

The total fields in the waveguide are defined as $(\bar{E}^{\rm wg}, \bar{H}^{\rm wg}) = (\bar{E}^i, \bar{H}^i) + (\bar{E}^r, \bar{H}^r)$. Specifying the Fourier transform as

$$\tilde{f}(\xi,\eta) = \int_{-\infty}^{\infty}\int_{-\infty}^{\infty} f(x,y) e^{j(\xi x+\eta y)}\, dx\, dy \quad (11)$$

and its inverse transform as

$$f(x,y) = \frac{1}{4\pi^2}\int_{-\infty}^{\infty}\int_{-\infty}^{\infty} \tilde{f}(\xi,\eta) e^{-(\xi x+\eta y)}\, dx\, dy \quad (12)$$

and by substituting (7) and (8) into (9) and (10) and taking their Fourier transforms, we can solve for $A^{e,h}(\xi,\eta)$

$$A^e(\xi,\eta) = \frac{-k_1^2\left[\xi\tilde{E}^{\rm wg}_x(\xi,\eta) + \eta\tilde{E}^{\rm wg}_y(\xi,\eta)\right]}{\zeta(\xi^2+\eta^2)} \quad (13)$$

$$A^h(\xi,\eta) = \frac{-k_1\left[\eta\tilde{E}^{\rm wg}_x(\xi,\eta) - \xi\tilde{E}^{\rm wg}_y(\xi,\eta)\right]}{(\xi^2+\eta^2).} \quad (14)$$

To obtain all of the unknowns, the magnetic boundary conditions at the waveguide aperture must be satisfied as well, leading to

$$\begin{aligned} &\frac{1}{4\pi^2}\int_{-\infty}^{\infty}\int_{-\infty}^{\infty} \tilde{H}^t_{x,y}(\xi,\eta) e^{-j(\xi x+\eta y)}\, d\xi\, d\eta \\ &\quad = H^{\rm wg}_{x,y}(x,y,0) \\ &\quad = H^i_{x,y}(x,y,0) + H^r_{x,y}(x,y,0) \end{aligned} \quad (15)$$

where $|x| \leq a$ and $|y| \leq b$. Using the orthogonality properties of the basis functions (i.e., waveguide modes), we multiply both sides of (15) by $[\sin a_p(x+a)\cos b_q(y+b)]$ for the H_x component and by $[\cos a_p(x+a)\sin b_q(y+b)]$ for the H_y component and integrate over the aperture. In this fashion the following relationships are obtained:

$$\begin{aligned} &\frac{1}{4\pi^2}\int_{-\infty}^{\infty}\int_{-\infty}^{\infty} \tilde{H}^t_x(\xi,\eta) S^a_p(\xi) C^b_q(\eta)\, d\xi\, d\eta \\ &\quad = \int_{-a}^{a}\int_{-b}^{b} H^i_x(x,y,0) \sin a_p(x+a)\cos b_q(y+b)\, dx\, dy \\ &\qquad + \frac{jab}{k_o^2 Z_o}\left[A^e_{pq} b_q k_o - A^h_{pq} a_p k_{pq}(1+\delta_{0q})\right] \end{aligned} \quad (16)$$

for $p = 1,2,3,\ldots,\infty$, $q = 0,1,2,\ldots,\infty$, and

$$\begin{aligned} &\frac{1}{4\pi^2}\int_{-\infty}^{\infty}\int_{-\infty}^{\infty} \tilde{H}^t_y(\xi,\eta) C^a_p(\xi) S^b_q(\eta)\, d\xi\, d\eta \\ &\quad = \int_{-a}^{a}\int_{-b}^{b} H^i_y(x,y,0) \cos a_p(x+a)\sin b_q(y+b)\, dx\, dy \\ &\qquad - \frac{jab}{Z_o}\left[\frac{A^e_{pq} a_p}{k_o} + \frac{A^h_{pq} b_q k_{pq}(1+\delta_{0p})}{k_o^2}\right] \end{aligned} \quad (17)$$

for $p = 0,1,2,\ldots,\infty$, $q = 1,2,3,\ldots,\infty$ and the rest of the

variables in (16) and (17) are defined as

$$\delta_{pq} = \begin{cases} 1 & \text{if } p = q \\ 0 & \text{otherwise} \end{cases} \tag{18}$$

$$S_p^a(\xi) = \int_{-a}^{a} \sin a_p(x+a) e^{-j\xi x}\, dx \tag{19}$$

$$C_q^b(\eta) = \int_{-b}^{b} \cos b_q(y+b) e^{-j\eta y}\, dy \tag{20}$$

$$C_p^a(\xi) = \int_{-a}^{a} \cos a_p(x+a) e^{-j\xi x}\, dx \tag{21}$$

$$S_q^b(\eta) = \int_{-b}^{b} \sin b_q(y+b) e^{-j\eta y}\, dy. \tag{22}$$

Equations (19) through (22) can easily be solved for all cases of p and q.

The expressions for $\tilde{H}_{x,y}^t(\xi,\eta)$ are readily obtained from (7) and (8) using (13) and (14), and are given by

$$\tilde{H}_x^t(\xi,\eta) = \frac{-\left[\xi\eta\tilde{E}_x^{\text{wg}}(\xi,\eta) + \left(k_1^2 - \xi^2\right)\tilde{E}_y^{\text{wg}}(\xi,\eta)\right]}{\zeta k_1 \eta_1} \tag{23}$$

$$\tilde{H}_y^t(\xi,\eta) = \frac{\tilde{E}_x^{\text{wg}}(\xi,\eta)\left(k_1^2 - \eta^2\right) + \xi\eta\tilde{E}_y^{\text{wg}}(\xi,\eta)}{\zeta k_1 \eta_1}. \tag{24}$$

Substituting (23) and (24) and the expressions for $\tilde{E}_{x,y}^{\text{wg}}(\xi,\eta)$ into (16) and (17), we obtain two linear sets of equations that lead to the solution of the unknown coefficients A_{mn}^e and A_{mn}^h, given by

$$\begin{aligned} &\sum_{m,n=1}^{\infty} \left[a_m I_1(m,n,p,q) + b_n I_2(m,n,p,q)\right] \cdot k_{mn} A_{mn}^e \\ &\quad + \sum_{\substack{m,n=0 \\ m=n\neq 0}}^{\infty} \left[b_n I_1(m,n,p,q) - a_m I_2(m,n,p,q)\right] \cdot k_o A_{mn}^h \\ &\quad + k_o^2 ab \left[\frac{A_{pq}^e b_q}{k_o} - \frac{A_{pq}^h a_p k_{pq}(1+\delta_{0q})}{k_o^2}\right] \cdot \frac{\eta_1}{\eta_o} \\ &\quad = \left[k_o a_1 I_2(1,0,p,q) - 2k_{10} a_1 \frac{\eta_1}{\eta_o} ab\delta_{1p}\delta_{0q}\right] \cdot A^i \end{aligned} \tag{25}$$

where for $p = 1,2,3,\ldots,\infty$, $q = 0,1,2,\ldots,\infty$, and

$$\begin{aligned} &\sum_{m,n=1}^{\infty} \left[a_m I_3(m,n,p,q) + b_n I_4(m,n,p,q)\right] \cdot k_{mn} A_{mn}^e \\ &\quad + \sum_{\substack{m,n=0 \\ m=n\neq 0}}^{\infty} \left[b_n I_3(m,n,p,q) - a_m I_4(m,n,p,q)\right] \cdot k_o A_{mn}^h \\ &\quad + k_o^2 ab \left[\frac{A_{pq}^e a_p}{k_o} + \frac{A_{pq}^h b_q k_{pq}(1+\delta_{0p})}{k_o^2}\right] \cdot \frac{\eta_1}{\eta_o} \\ &\quad = \left[k_o a_1 I_4(1,0,p,q)\right] \cdot A^i \end{aligned} \tag{26}$$

for $p = 0,1,2,\ldots,\infty$, $q = 1,2,3,\ldots,\infty$ and where the $I_{n=1,2,3,4}(m,n,p,q)$ integrals are as

$$\begin{aligned} I_1(m,n,p,q) &= \frac{1}{4\pi^2} \int_{-\infty}^{\infty}\int_{-\infty}^{\infty} \frac{\xi\eta}{\zeta k_1} C_m^a(-\xi) S_n^b(-\eta) \\ &\quad \times S_p^a(\xi) C_q^b(\eta)\, d\eta\, d\xi \end{aligned} \tag{27}$$

TABLE I
VALUES OF (m,n) OF MODES IN NUMERICAL CALCULATION

Number of Modes	TE_{mn}	TM_{mn}
1	(1,0)	———
6	(1,0); (3,0); (1,2); (3,2)	(1,2); (3,2)
15	(1,0); (3,0); (5,0); (1,2); (1,4); (3,2); (3,4); (5,2); (5,4);	(1,2); (1,4); (3,2); (3,4); (5,2); (5,4);
20	(1,0); (3,0); (5,0); (7,0); (1,2); (1,4); (3,2); (3,4); (5,2); (5,4); (7,2); (7,4)	(1,2); (1,4); (3,2); (3,4); (5,2); (5,4); (7,2); (7,4)

$$\begin{aligned} I_2(m,n,p,q) &= \frac{1}{4\pi^2} \int_{-\infty}^{\infty}\int_{-\infty}^{\infty} \frac{\left(k_1^2 - \xi^2\right)}{\zeta k_1} S_m^a(-\xi) C_n^b(-\eta) \\ &\quad \times S_p^a(\xi) C_q^b(\eta)\, d\eta\, d\xi \end{aligned} \tag{28}$$

$$\begin{aligned} I_3(m,n,p,q) &= \frac{1}{4\pi^2} \int_{-\infty}^{\infty}\int_{-\infty}^{\infty} \frac{\left(k_1^2 - \eta^2\right)}{\zeta k_1} C_m^a(-\xi) S_n^b(-\eta) \\ &\quad \times C_p^a(\xi) S_q^b(\eta)\, d\eta\, d\xi \end{aligned} \tag{29}$$

$$\begin{aligned} I_4(m,n,p,q) &= I_1(p,q,m,n) \\ &= \frac{1}{4\pi^2} \int_{-\infty}^{\infty}\int_{-\infty}^{\infty} \frac{\xi\eta}{\zeta k_1} S_m^a(-\xi) C_n^b(-\eta) \\ &\quad \times C_p^a(\xi) S_q^b(\eta)\, d\eta\, d\xi. \end{aligned} \tag{30}$$

The modified expressions for (26)–(29) and considerations for their numerical evaluation are presented in Appendix A which result in a double integration over the aperture of the waveguide (bounded integrals) containing simple trigonometric functions without singularities in the integrand. The choice of basis function (higher-order modes) used in the solution are also discussed. The solution for A_{mn}^e and A_{mn}^h is then simply dependent on solving $I_{n=1,2,3,4}(m,n,p,q)$ integrals and on the truncated linear set of equations. This truncation does not constitute a numerical approximation but a limit to which the contribution of any additional higher-order modes becomes insignificant (i.e., convergence). Because of the even geometry of the problem, only modes possessing odd m and even n indices will be coupled with the incident TE_{10} mode. This behavior can be easily observed from the mathematical expression for $I_{n=1,2,3,4}(m,n,p,q)$ integrals in Appendix A. Also, since the TE_{mn} and TM_{mn} modes are coupled, it is explicit in (25) and (26) that for given (m,n) indices both modes must be included in the solution so that there is an equal number of equations and unknowns. A more intuitive explanation resides in the fact that since all the coupled modes are degenerate (i.e., same cutoff frequency), they have an equal likelihood of being generated and must be considered in the solution.

III. NUMERICAL RESULTS

The study of the open-ended waveguide discontinuity and its reflection properties theoretically involves an infinite expansion in (16) and (17). In this study, these equations will be solved by considering a limited set of basis function (1, 6, 15, and 20 waveguide modes) given in Table I. Unless otherwise specified, the results are for an infinite-half space of free-space. It will be further shown that the use of 6 higher-order

TABLE II
A^e_{mn} AND A^h_{mn} VALUES ($A^i = 1$) AT $f = 9.5$ GHz

Mode		[20]		This study	
		Amp.	Phase (deg.)	Amp	Phase (deg.)
TM_{12}	A^e_{12}	0.02273	-120.29	0.02256	-120.72
TM_{14}	A^e_{14}	0.00377	-116.47	0.00367	-117.037
TM_{32}	A^e_{32}	0.00165	-163.12	0.00165	-163.28
TM_{34}	A^e_{34}	0.00030	-164.13	0.00029	-164.39
TM_{52}	A^e_{52}	0.00061	-155.38	0.00061	-155.54
TM_{54}	A^e_{54}	0.00013	-155.82	0.00013	-156.12
TE_{10}	A^h_{10}	0.24178	-73.87	0.24564	-73.82
TE_{12}	A^h_{12}	0.01142	-17.75	0.01126	-18.12
TE_{14}	A^h_{14}	0.00210	-16.97	0.00201	-17.37
TE_{30}	A^h_{30}	0.01854	-65.32	0.01849	-65.67
TE_{32}	A^h_{32}	0.00082	-158.68	0.00084	-161.13
TE_{34}	A^h_{34}	0.00016	-129.43	0.00016	-135.23
TE_{50}	A^h_{50}	0.00442	-53.30	0.00437	-53.83
TE_{52}	A^h_{52}	0.00025	-179.72	0.00027	177.16
TE_{54}	A^h_{54}	0.00005	-136.22	0.00005	-149.64

modes is sufficient to achieve convergence. The following numerical procedure was performed in the X-band frequency range (8.2–12.4 GHz).

A. Convergence of A^h_{10} Coefficient

The solution for the reflection properties of the open-ended waveguide, as previously established, is solely dependent on the number of modes considered. The measurable parameter, that is the reflected portion of the dominant TE_{10} mode A^h_{10}, is computed for $A^i = 1$ and for the different number of modes listed in Table I. The results obtained for the case of 20 modes is used as a reference for which final convergence to the solution is assumed. Figs. 2 and 3 show the percent error of the magnitude and phase of the A^h_{10} coefficient for the case of one, six, and 15 modes with respect to the case of 20 modes as a function of frequency. The computation time for such a procedure on a 133 MHz Pentium processor is 0.38, 8.35, 47.84, and 83.54 s, respectively. It is seen that when using six or more modes, the difference with respect to the final solution is less than 1%. Thus, for practical and computational considerations, only six modes will be used hereafter to calculate the reflection coefficient Γ.

B. Calculation of the $A^{e,h}_{mn}$ Coefficients

To verify the results of this full wave integral formulation, the values of A^e_{mn} and A^h_{mn} for 15 modes of the reflected fields were calculated for $A^i = 1$ and compared to those obtained in [20], as shown in Table II. Considering an incident TE_{10} mode, the reflection coefficient Γ is simply the computed value of A^h_{10}. The other terms correspond to the presence of evanescent higher-order modes necessary to represent the complete field

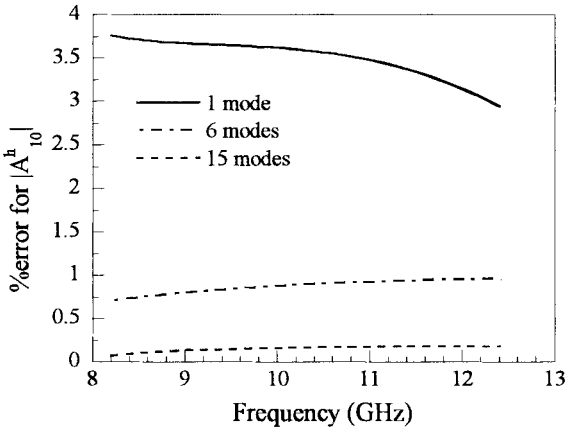

Fig. 2. Percent error for the magnitude of A^h_{10} coefficient as a function of the number of modes considered from Table I as a function of frequency.

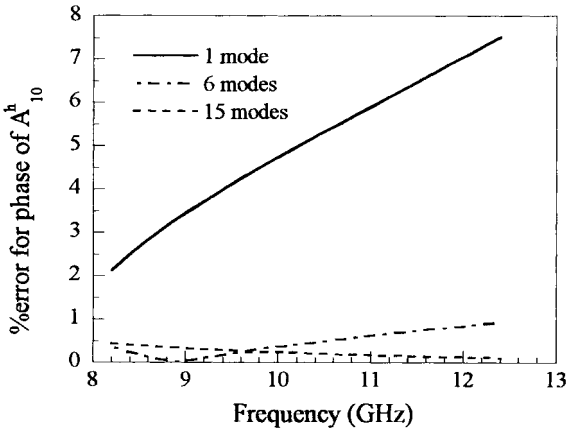

Fig. 3. Percent error for the phase of A^h_{10} coefficient as a function of the number of modes considered from Table I as a function of frequency.

distribution at the aperture. The results shown in Table II indicate a very good agreement between this exact solution and that used in [20]. Although some slight discrepancies exists, the present results are favored since they are computed using closed form integrals as opposed to the truncated and approximated integrals used in [20].

To interpret the order of importance of the contribution of the higher-order modes, one must first understand the physical mechanism under which they are created. The dominant mode has obvious predominance since it constitutes the exciting incident wave. This mode also generates TE_{m0} mode with odd m index because of the even geometry of the problem. The other higher-order mode components of the solution are modal harmonics of the TM_{12} and TE_{12} modes. The mechanism of the generation of the TM_{12} and TE_{12} modes is consistent with the fringing of the fields in the y-direction outside the waveguide. It is also the lowest (m, n) subset and therefore their amplitudes will be greater than that of the higher harmonics (i.e., $m = 3, 5 \cdots$ and $n = 2, 4, \cdots$).

Because of the null field distribution of the TE_{10} mode at the waveguide walls in the x-direction (at $x = -a$ and $x = a$), the change in the medium of propagation (i.e., bounded to unbounded) does not present a significant discontinuity. On the

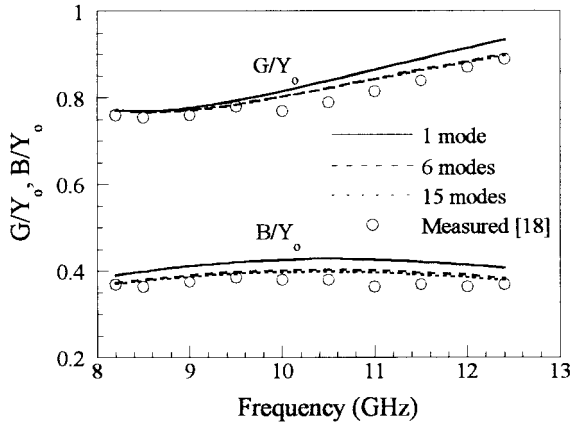

Fig. 4. Normalized admittance as a function of frequency for one mode (solid line), six modes (dashed), 15 modes (dotted), measured [18] (circles).

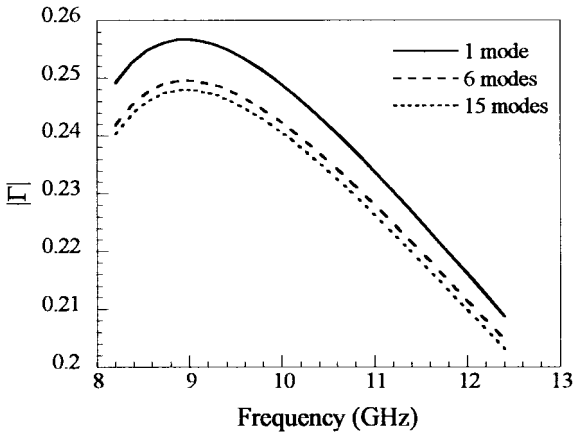

Fig. 5. Magnitude of reflection coefficient as a function of frequency for one, six, and 15 modes.

other hand, the fields are constant in the y-direction over the vertical dimension of the waveguide right before the aperture $(z = 0^-)$. Because of the boundary condition set by the perfectly conducting flange, fringing of the fields will occur. As shown in [26], in which the near-field patterns of the open-ended waveguide radiating into a dielectric half-space were computed, the presence of side-lobes in this direction would require the contribution of the TM_{12} mode to better represent the fields at the aperture of the waveguide.

C. Variation of the Aperture Admittance (Y) and the Reflection Coefficient (Γ) as a Function of Frequency for Different Number of Basis Functions

Fig. 4 shows the frequency dependence of the normalized aperture admittance given by

$$Y_n = \frac{Y}{Y_o} = \frac{A^i - A^h_{10}}{A^i + A^h_{10}} \tag{31}$$

where $Y_o = k_{10}/\omega\mu_o$ is the characteristic admittance of the incident TE_{10} mode.

The results for 1, 6 and 15 modes are compared to the measured values obtained in [18], and clearly good agreement is obtained. It can be inferred by the convergence of the solution for Y_n that six modes are sufficient to adequately represent the field distribution at the aperture. Also, it can be seen that although there is a quasiconstant difference between the multimode and dominant mode solutions for B/Y_o as a function of frequency, the solutions for G/Y_o actually diverge.

Therefore, the contribution of the higher-order modes varies as a function of the frequency of the exciting wave in a given waveguide band (or as a function of a/λ_o) which is an important issue. Figs. 5 and 6 present the magnitude and phase of the reflection coefficient as a function of frequency for the three previous modal solutions, respectively. As discussed, the contribution of the higher-order modes is shown to be frequency dependent and is more prominent in the higher portion of the operating frequency band.

To better illustrate the frequency dependence of the contribution of the higher-order modes, the magnitude of $A^{e,h}_{mn}$ coefficients are plotted in Fig. 7 as a function of frequency for

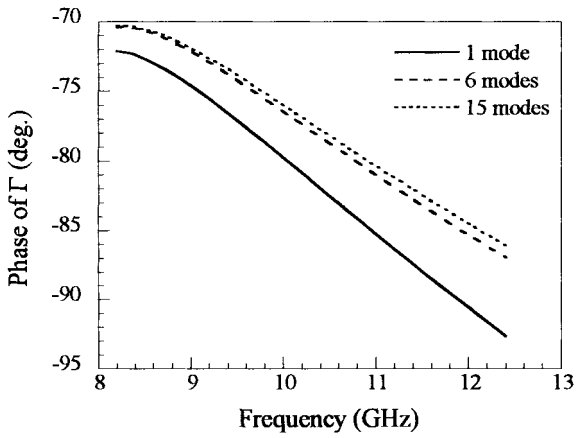

Fig. 6. Phase of reflection coefficient as a function of frequency for one, six, and 15 modes.

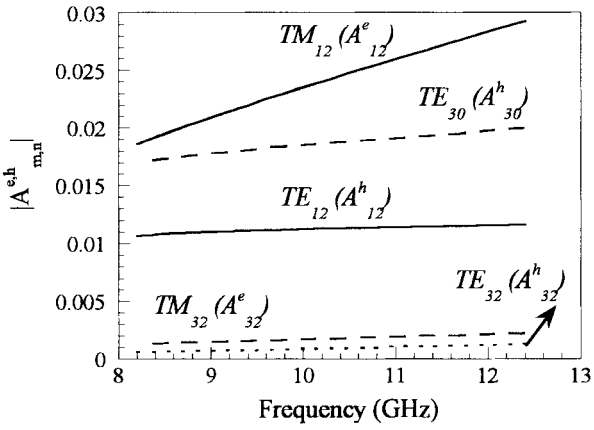

Fig. 7. Magnitude of higher-order modes for the case of free-space as a function of frequency.

the six different modes shown in Table I. The increase in the contribution of the higher-order modes is due to the fact that as the frequency increases the waveguide operates at frequencies that are increasingly closer to the cutoff frequencies of these modes. In light of the results shown in Fig. 7, the significant increase in the contribution of the TM_{12} mode leads us to believe that the variational expressions used in [13] and [14]

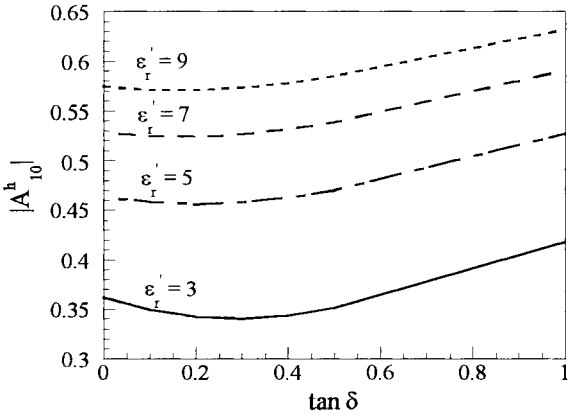

Fig. 8. Magnitude of reflected dominant TE_{10} mode at $f = 12.4$ GHz as a function of varying dielectric properties.

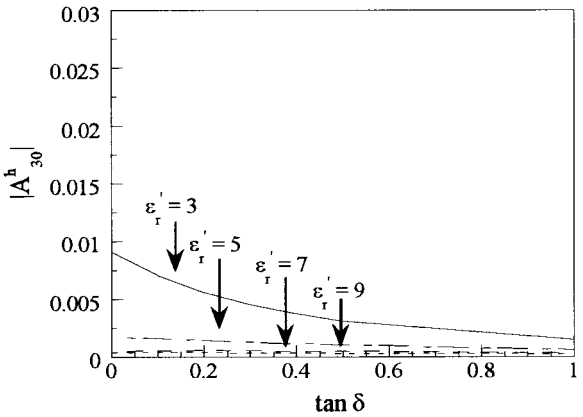

Fig. 10. Magnitude of reflected TE_{30} mode at $f = 12.4$ GHz as a function of varying dielectric properties.

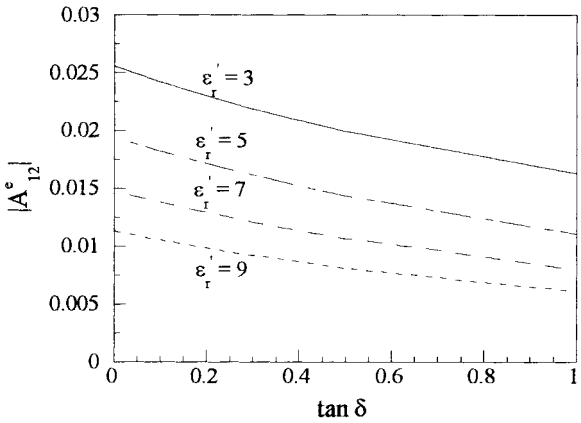

Fig. 9. Magnitude of reflected TM_{12} mode at $f = 12.4$ GHz as a function of varying dielectric properties.

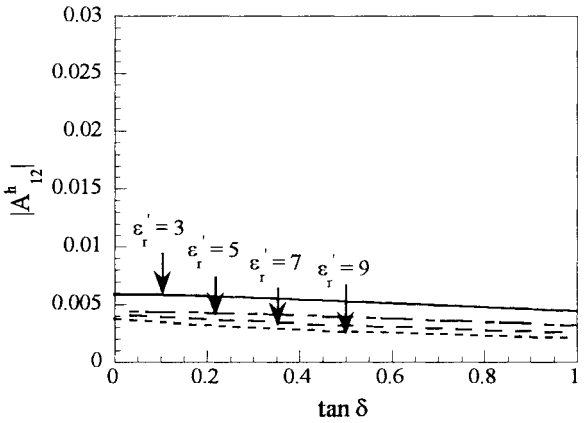

Fig. 11. Magnitude of reflected TE_{12} mode at $f = 12.4$ GHz as a function of varying dielectric properties.

breakdown as the frequency increases within the waveguide operating frequency band. From a swept frequency dielectric property measurement perspective, the discrepancy between the dominant and multimode solutions translates into the misinterpretation that the dielectric properties change as a function of frequency (within the waveguide band) even though they may be constant throughout the swept frequency range.

D. Variation of the Reflection Coefficient (Γ) *as a Function of the Dielectric Properties of the Infinite Half-Space*

Since the focal point of this study is to better characterize the open-ended waveguide probe as a tool for nondestructive dielectric property measurements, the behavior of the multimode solution of the aperture admittance and reflection properties as a function of the relative permittivity and loss tangent of the dielectric infinite half-space must be discussed as well. Calculations of the $A^{e,h}_{mn}$ coefficients were performed using six modes for different values of ε_r' (three, five, seven, and nine) and $\tan\delta = \varepsilon_r''/\varepsilon_r'$ (0.0, 0.1, 0.2, 0.3, 0.4, 0.5, and 1.0) at a frequency of 12.4 GHz where the influence of the higher-order modes is shown to be most pronounced (see Fig. 7). Figs. 8–11 present the magnitude of the four most significant modes as a function of ε_r. It is worth noting that the magnitude of reflection coefficient (A^h_{10}) increases for an increasing ε_r' but the contribution of the higher-order modes decreases as a function of this parameter. This means that for a high enough ε_r', the contribution of the higher-order modes to the amplitude of the reflected portion of the dominant mode is quite minimal so that the variational approximation may be sufficient to adequately calculate Γ. In this case, the fringing of the fields at the aperture, which was previously identified as a mechanism for the generation of higher-order modes, is minimized so that the field distribution converges to that of the dominant TE_{10} mode. This feature emphasizes that in previous studies such as in [5], where the material under test possessed sufficiently large ε_r' (i.e., rubber compounds), the obtained experimental results would be similar to those obtained with the use of this new exact multimode solution.

IV. Inverse Problem

In [11] and [12], dielectric property measurements of cement based materials (e.g., mortar which is composed of water, cement powder and sand) using open-ended rectangular waveguides were performed using the single mode approximation. In this instance it was assumed that when modeling the forward problem (i.e., calculating Γ from ε_r), only the dominant TE_{10} mode was included in the solution. When

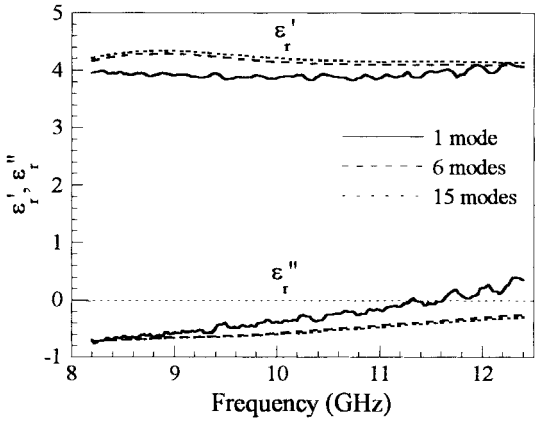

Fig. 12. Calculated values of the complex dielectric constant of mortar at X-band using one (solid line), six (dashed line), and 15 (dotted) waveguide modes (the thin line indicates zero).

attempting the inverse problem (i.e., calculating ε_r from Γ), the limitations of this model became apparent when the computed imaginary part of the dielectric properties, ε_r'', yielded positive results in the higher portion of the waveguide frequency band (see the solid line of Fig. 12). This result was obviously wrong since it implied that the electromagnetic wave increased in amplitude (and power) as it propagated in the lossy medium. In the theoretical section, its was shown that using 6 waveguide modes were sufficient (namely, TE_{10}, TE_{12}, TM_{12}, TE_{30}, TE_{32} and TM_{32}) to adequately represent the fields at the aperture of an open-ended rectangular waveguide radiating into a dielectric infinite half-space. Using this new formulation, the inversion scheme was repeated for the same set of data used to produce the single mode solution of Fig. 12. To do so, a multisecant [27] root-solving scheme was used in conjunction with a convergence check. In addition, the calculations were also repeated for 15 waveguide modes (TE_{mn} and TM_{mn} modes are enumerated in Table I) to verify the convergence of the solution.

Using this scheme and the measured reflection coefficient, the dielectric properties of mortar was calculated and presented in Fig. 12. It can be seen that the measured values for the loss factor ε_r'' are always negative and thus yielded physically meaningful results. Also, increasing the number of modes from six to 15 did not significantly influence the outcome of the final solution for ε_r. This would indicate that for measuring of the dielectric constant of cementious materials, six waveguide modes are sufficient. Finally, the results are much more linear as a function of frequency using the higher-order mode formulation. This behavior agrees with the modeling of the behavior of ε_r versus frequency using a single pole linear system over a relatively narrow frequency band [28].

V. Conclusion

A full wave formulation describing the behavior of the reflection properties of an open-ended waveguide radiating into a dielectric half-space is presented in this paper. The theoretical formulation for the problem is simple, thorough and non-approximate in which only a set of simple 2-D integrals must be numerically computed. The computation time for such a procedure on a 133 MHz Pentium processor is about 8 s when using six modes and 48 s when using 15 modes. The derivations of the said reflection properties are performed through Fourier analysis with proper boundary matching and include cross-polarization by incorporating both the electric and magnetic Hertzian vector potentials. The only accuracy dependant factor is the choice of the number of modes used in the solution. It was shown that only six modes are necessary to achieve accuracy to within 1% of the final solution (e.g., using 20 modes) for the magnitude and the phase of the reflection coefficient. Since the practical implementation of the present work lies in its inverse problem (i.e., retrieving the dielectric properties of the half-space from the measured reflection properties), which requires a numerical root-solving technique, minimizing the number of required higher-order modes used in the solution is therefore computationally advantageous.

It has also been shown that the contribution of the higher-order modes is frequency and dielectric property dependent. This contribution is more pronounced in the higher portion of the operating frequency range of a waveguide band and for low permittivity and low loss materials. Because of this behavior, variational methods that only include the influence of the dominant mode may produce satisfactory reflection property measurement results for a given range of frequencies (in the lower portion of a waveguide band) and high enough dielectric property values.

The new derivation was used for the inverse problem, in which the dielectric constant of an infinite dielectric half-space of mortar was calculated from reflection coefficient measurement. The dielectric properties of a mortar specimen previously considered in [10] was recalculated using six modes. It was shown that the inclusion of five higher-order modes (TE_{12}, TM_{12}, TE_{30}, TE_{32}, and TM_{32}) was sufficient to adequately represent the fields at the aperture of an open-ended rectangular waveguide radiating into a dielectric infinite half-space. Using the multimode solution yielded physically meaningful results.

Appendix

Reduced Expressions for $I_{n=1,2,3,4}(m,n,p,q)$ Integrals

The integrals are described as

$$I_1(m,n,p,q) = \frac{1}{4\pi^2}\int_{-\infty}^{\infty}\int_{-\infty}^{\infty}\frac{\xi\eta}{\zeta k_1}C_m^a(-\xi)S_n^b(-\eta) \times S_p^a(\xi)C_q^b(\eta)\,d\eta\,d\xi \tag{A1}$$

$$I_2(m,n,p,q) = \frac{1}{4\pi^2}\int_{-\infty}^{\infty}\int_{-\infty}^{\infty}\frac{(k_1^2-\xi^2)}{\zeta k_1}S_m^a(-\xi)C_n^b(-\eta) \times S_p^a(\xi)C_q^b(\eta)\,d\eta\,d\xi \tag{A2}$$

$$I_3(m,n,p,q) = \frac{1}{4\pi^2}\int_{-\infty}^{\infty}\int_{-\infty}^{\infty}\frac{(k_1^2-\eta^2)}{\zeta k_1}C_m^a(-\xi)S_n^b(-\eta) \times C_p^a(\xi)S_q^b(\eta)\,d\eta\,d\xi \tag{A3}$$

$$I_4(m,n,p,q) = I_1(p,q,m,n) = \frac{1}{4\pi^2}\int_{-\infty}^{\infty}\int_{-\infty}^{\infty}\frac{\xi\eta}{\zeta k_1}S_m^a(-\xi)C_n^b(-\eta) \times C_p^a(\xi)S_q^b(\eta)\,d\eta\,d\xi. \tag{A4}$$

Each is in the form of

$$I_n(m,n,p,q) = \frac{1}{4\pi^2}\int_{-\infty}^{\infty}\int_{-\infty}^{\infty}\frac{\hat{f}_n(\xi,\eta)}{\sqrt{k_1^2-\xi^2-\eta^2}}\,d\eta\,d\xi. \tag{A5}$$

Using Parseval's theorem given as

$$\int_{-\infty}^{\infty}\int_{-\infty}^{\infty} g_1(x,y)g_2(-x,-y)\,dx\,dy = \frac{1}{4\pi^2}\int_{-\infty}^{\infty}\int_{-\infty}^{\infty}\tilde{g}_1(\xi,\eta)\tilde{g}_2(\xi,\eta)\,d\eta\,d\xi \tag{A6}$$

we can separate the integrand into two separate functions and take their respective inverse Fourier transforms where

$$g_1(x,y) = \frac{1}{4\pi^2}\int_{-\infty}^{\infty}\int_{-\infty}^{\infty}\tilde{f}_n(\xi,\eta)e^{-j(\xi x+\eta y)}\,d\eta\,d\xi \tag{A7}$$

$$g_2(x,y) = \frac{1}{4\pi^2}\int_{-\infty}^{\infty}\int_{-\infty}^{\infty}\frac{e^{-j(\xi x+\eta y)}}{\sqrt{k_1^2-\xi^2-\eta^2}}\,d\eta\,d\xi. \tag{A8}$$

The final expression of (A8) is given in [13] as

$$g_2(x,y) = \frac{j}{2\pi}\frac{e^{-jk_1\sqrt{x^2+y^2}}}{\sqrt{x^2+y^2}} = g_2(-x,-y) \tag{A9}$$

It should be noted that (A9) is an even function and that the $\tilde{f}_n(\xi,\eta)$ will be either an odd or even function with respect to the ξ and η axis depending on the choice of m, n, p and q. Due to the properties of the Fourier transforms, the inverse Fourier transforms of $\tilde{f}_n(\xi,\eta)$ will possess the same even and odd behaviors. Therefore, (A6) is zero whenever $\tilde{f}_n(\xi,\eta)$ is odd with respect to either the ξ and η axis. This is the case whenever p or m are even and q or n are odd. This mathematically supports the physical hypothesis that only modes possessing odd m and even n indices will be coupled with the incident TE_{10} mode. This fact is not explicitly described in most studies on the subject.

The expressions for $g_1(x,y)$ (inverse Fourier transforms) can be easily computed and will not be derived in this paper. The point of interest is that $g_1(x,y)$ is defined over the aperture area and zero elsewhere for all cases. Therefore

$$I_n(m,n,p,q) = \frac{j}{2\pi}\int_0^a\int_0^b\frac{g_1(x,y)e^{-jk_1\sqrt{x^2+y^2}}}{\sqrt{x^2+y^2}}\,dy\,dx. \tag{A10}$$

This expression can easily be evaluated via a Gauss–Legendre [24] quadrature method in this singular form since the function is never evaluated at the singularity and the weight associated to the function evaluation at points close to $x=y=0$ are very small. The singularity in the $I_{n=1,2,3,4}(m,n,p,q)$ integrals can be easily removed by switching to polar coordinates although this increases the computation time by twofold since the integral has to be divided into two regions.

ACKNOWLEDGMENT

The authors wish to thank K. Yoshitomi for his invaluable discussions and generous support in providing comparative results during the theoretical phase of this study.

REFERENCES

[1] M. C. Decreton and F. E. Gardiol, "Simple nondestructive method for measurement of complex permittivity," *IEEE Trans. Instrum. Meas.*, vol. IM-23, pp. 434–438, Dec. 1974.
[2] M. C. Decreton and M. S. Ramachandraiah, "Nondestructive measurement of complex permittivity for dielectric slabs," *IEEE Trans. Microwave Theory Tech.*, vol. MTT-23, pp. 1077–1080, Dec. 1975.
[3] V. Teodoris, T. Sphicopoulos, and F. E. Gardiol, "The reflection from an open-ended waveguide terminated by a layered dielectric medium," *IEEE Trans. Microwave Theory Tech.*, vol. MTT-33, pp. 359–366, May 1985.
[4] B. A. Sanadiki and M. Mostafavi, "Inversion of homogeneous continuously varying dielectric profiles using open-ended waveguides," *IEEE Trans. Antennas Propagat.*, vol. 39, pp. 158–163, Feb. 1991.
[5] S. I. Ganchev, S. Bakhtiari, and R. Zoughi, "A novel numerical technique for dielectric measurement of generally lossy dielectrics," *IEEE Trans. Instrum. Meas.*, vol. 41, pp. 361–365, June 1992.
[6] S. Bakhtiari, N. Qaddoumi, S. Ganchev, and R. Zoughi, "Microwave noncontact examination of disbond and thickness variation in stratified composite media," *IEEE Trans. Microwave Theory Tech.*, vol. 42, pp. 389–395, Mar. 1994.
[7] N. Qaddoumi, R. Zoughi, and G. W. Carriveau, "Microwave detection and depth determination of disbonds in low-permittivity and low-loss thick sandwich composites," *Res. Nondestruct. Eval.*, vol. 8, no. 1, pp. 51–63, 1996.
[8] S. Gray, S. Ganchev, N. Qaddoumi, G. Beauregard, D. Radford, and R. Zoughi, "Porosity level estimation in polymer composites using microwaves," *Mater. Eval.*, vol. 53, no. 3, pp. 404–408, 1995.
[9] C. Huber, H. Abiri, S. Ganchev, and R. Zoughi, "Analysis of the crack characteristic signal using a generalized scattering matrix representation," *IEEE Trans. Microwave Theory Tech.*, vol. 45, pp. 477–484, Apr. 1997.
[10] K. J. Bois, R. Mirshahi, and R. Zoughi, "Dielectric mixing models for cement based materials," in *Proc. Review Progress Quantitative NDE*. New York: Plenum, 1997, vol. 16A, pp. 657–663.
[11] K. J. Bois, A. D. Benally, P. S. Nowak, and R. Zoughi, "Cure-state monitoring and early water-to-cement (w/c) determination of portland cement based materials using near-field microwave techniques," *IEEE Trans. Instrum. Meas.*, vol. 47, pp. 628–637, June 1998.
[12] K. Nikita and N. Uzunoglu, "Analysis of the power coupling from a waveguide hyperthermia applicator into a three-layered tissue model," *IEEE Trans. Microwave Theory Tech.*, vol. 37, pp. 1794–1800, Nov. 1989.
[13] L. Lewin, *Advance Theory of Waveguides*. London, U.K.: Iliffe, 1951.
[14] R. T. Compton, "The admittance of aperture antennas radiating into lossy media," Ph.D. dissertation, Ohio State Univ., Columbus, 1964.
[15] R. J. Mailloux, "Radiation and near field coupling between two colinear open ended waveguides," *IEEE Trans. Antennas Propagat.*, vol. AP-17, pp. 49–55, Jan. 1969.
[16] ———, "First order solution for mutual coupling between two collinear open ended waveguides," *IEEE Trans. Antennas Propagat.*, vol. AP-17, pp. 740–746, Nov. 1969.
[17] J. R. Mautz and R. F. Harrington, "Transmission from a rectangular waveguide into half-space through a rectangular aperture," *IEEE Trans. Microwave Theory Tech.*, vol. MTT-26, pp. 44–45, Jan. 1978.
[18] D. G. Bodnar and D. T. Paris, "New variational principle in electromagnetics," *IEEE Trans. Antennas Propagat.*, vol. AP-18, pp. 216–223, Mar. 1970.
[19] A. R. Jamieson and T. E. Rozzi, "Rigorous analysis of cross polarization in flange-mounted rectangular waveguide radiators," *Electron. Lett.*, vol. 13, pp. 742–744, Nov. 24, 1977.
[20] K. Yoshitomi and H. R. Sharobim, "Radiation from a rectangular waveguide with a lossy flange," *IEEE Trans. Antennas Propagat.*, vol. 42, pp. 1398–1403, Oct. 1994.
[21] R. H. MacPhie and A. I. Zaghloul, "Radiation from a rectangular waveguide with infinite flange-exact solution by the correlation matrix," *IEEE Trans. Antennas Propagat.*, vol. AP-28, pp. 497–503, July 1980.
[22] H. Baudrand, J. W. Tao, and J. Atechian, "Study of radiating properties of open-ended waveguides," *IEEE Trans. Antennas Propagat.*, vol. 36, pp. 1071–1077, Aug. 1988.
[23] C. W. Chang, K. M. Chen, and J. Qian, "Nondestructive determination of electromagnetic parameters of dielectric materials at X-band frequencies using a waveguide probe system," *IEEE Trans. Instrum. Meas.*, vol. 46, pp. 1084–1092, Oct. 1997.
[24] ———, "Nondestructive measurement of complex tensor permittivity of anisotropic materials using a waveguide probe system," *IEEE Trans. Microwave Theory Tech.*, vol. 44, pp. 1081–1090, July 1997.

[25] A. Ishimaru, *Electromagnetic Wave Propagation, Radiation, and Scattering*. Englewood Cliffs, NJ: Prentice-Hall, 1991, pp. 20–23.
[26] N. Qaddoumi, H. Abiri, S. Ganchev, and R. Zoughi, "Near-field analysis of rectangular probes used for imaging," in *Proc. Review Progress Quantitative NDE*. New York: Plenum, 1995, vol. 15A, pp. 727–732.
[27] W. H. Press, B. P. Flannery, S. A. Teukolsky, and W. T. Vetterling, *Numerical Recipes*, 2nd Ed. Cambridge, U.K.: Cambridge Univ. Press, 1992.
[28] J. Baker-Jarvis, M. D. Janezic, J. H. Grosvenor, and R. G. Geyer, "Transmission/reflection and short-circuit line methods for measuring permittivity and permeability," NIST Tech. Note 1355-R, U.S. Dept. Commerce, Boulder, CO, pp. 52–57, Dec. 1993.

Karl J. Bois (M'93) received the B.Sc. and M.Sc. degrees in electrical engineering from the Université Laval, Québec, P.Q., Canada, in 1993 and 1995, respectively. He received the Ph.D. degree in electrical engineering from Colorado State University (CSU), Fort Collins, in 1999.

From 1995 to 1999, while at the Applied Microwave Nondestructive Testing Laboratory, CSU, his main areas of research involved microwave nondestructive characterization of cement based materials, developing new techniques for measuring the electrical properties of materials, and exploring novel theoretical formulae for the near-field characteristics of open-ended rectangular waveguides. He s currently with the Packaging Group, VLSI Technology Center, Hewlett-Packard Company, Fort Collins. His main functions include EMI and signal integrity modeling efforts for next generation computer chip packages, and implementing test benches for experimental verification.

Aaron D. Benally received the B.Sc. degree in electrical engineering from Colorado State University, Fort Collins.

He is currently conducting research in nondestructive inspection and monitoring of concrete structures using microwave near-field techniques.

Reza Zoughi (M'86–SM'93) received the B.S.E.E., M.S.E.E., and Ph.D. degrees in electrical engineering (radar remote sensing, radar systems, and microwaves) from the University of Kansas, Lawrence.

From 1981 to 1987, he was with the Radar Systems and Remote Sensing Laboratory, University of Kansas. He has been at Colorado State University (CSU), Fort Collins, since 1987, where he is now a Professor of electrical and computer engineering, where he established the Applied Microwave Nondestructive Testing Laboratory. His current areas of research include nondestructive testing of material using microwaves, developing new techniques for microwave and millimeter wave inspection and testing of materials and developing new electromagnetic probes to measure characteristic properties of material at microwave frequencies. He has over 200 journal publications, conference presentations and proceedings, technical reports, and overview articles in the fields of radar remote sensing and microwave nondestructive evaluation. He is also the co-inventor on four patents in the field of microwave nondestructive testing and evaluation.

Dr. Zoughi has been voted the most outstanding teaching faculty seven times by the junior and senior students in the Electrical and Computer Engineering Department, CSU. He has also been recognized as an honored researcher four times by the CSU Research Foundation. He was the recipient of the Dean's Council Award in 1992, and the Abell Faculty Teaching Award in 1995. He was also the Business Challenge Endowment Associate Professor of Electrical and Computer Engineering (1995–1997). He is the 1996 recipient of the Colorado State Board of Agriculture Excellence in Undergraduate Teaching Award. He is a senior member of Sigma Xi, Eta Kappa Nu, and the American Society for Nondestructive Testing. He is an Associate Technical Editor for the IEEE TRANSACTIONS ON INSTRUMENTATION AND MEASUREMENT and *Materials Evaluation* and served as the Guest Associate Editor for the Special Microwave NDE Issue of *Research in Nondestructive Evaluation* in 1995 and the Special Microwave Issue of *Materials Evaluation* in 1994.